Available online at www.sciencedirect.com
ScienceDirect
Journal of Photochemistry and Photobiology A: Chemistry 186 (2007) 106–114
Journal of Photochemistry and Photobiology A:Chemistry
www.elsevier.com/locate/jphotochem

Highly efficient sulfur-containing polymeric photoinitiators bearing side-chain benzophenone and coinitiator amine for photopolymerization

Hongyu Wang, Jun Wei, Xuesong Jiang, Jie Yin*

Research Institute of Polymer Materials, School of Chemistry & Chemical Technology, State Key Laboratory for Composite Materials,
Shanghai Jiao Tong University, Shanghai 200240, People's Republic of China

Received 9 May 2006; received in revised form 5 July 2006; accepted 27 July 2006

Abstract

Novel polymeric sulfur-containing photoinitiators bearing side-chain benzophenone and coinitiator amine, copolymers of 4-[(4-methacrylamido)thiophenyl]benzophenone (MAATPBP) and of 4-chloro-4′-[(4-methacrylamido)thiophenyl]benzophenone (CMAATPBP) with *N*,*N*-dimethylaminoethyl methacrylate (DMAEMA), as well as their hompolymers of poly(MAATPBP), poly(CMAATPBP) and poly(DMAEMA) were prepared and structurally characterized. The most commercially used photoinitiator BP and their corresponding low molecular weight combinations (MAATPBP/DMAEMA and CMAATPBP/DMAEMA) were selected as the reference to evaluate their photoefficiency. Polymeric photoinitiators display similar UV–vis maximal absorption spectra to the low molecular counterparts, which are greatly red-shifted in comparison with BP. Photopolymerization of difunctional 1,6-hexanediol diacrylate (HDDA) and trifunctional trimethylolpropane triacrylate (TMPTA) were studied by photo-DSC to investigate the photoefficiency of the copolymers, homopolymers and the combination of their homopolymers. The results show surprising high efficiency of the two copolymeric photoinitiators and their homopolymeric combinations. Poly(MAATPBP) and poly(CMAATPBP) can also efficiently initiate the photopolymerization without the coinitiator because of the photolysis at C–S bond. Their activity data obtained are discussed and related to the structural requirements of the above systems.

Keywords: Polymeric photoinitiator; Photopolymerization; Sulfur-containing initiator; Benzophenone

1. Introduction

Polymeric photoinitiators have recently gained an increasing interest [1–12] for their extensive applications in the field of printed circuits, encapsulation of electronic components, coatings, printing inks, and so forth. Their higher cost with respect to the corresponding low molecular weight analogues should, however, be justified by various advantages [13], such as nonyellowing, low-odor, compatibility improvement with formulation components as well as of lower contaminant release. Polymeric photoinitiators can be defined as macromolecular systems that contain pendent or in-chain chromophores [4], which absorb light efficiently and generate radicals capable of initiating polymerization. Conventionally, these photoinitiators have been classified into two main types: photofragmenting (type I photoinitiators) or hydrogen-abstracting chromophores (type II photoinitiators) [4]. Most of type II polymeric photoinitiators are based on benzophenone (BP) [4,13–15], probably because of its relatively low cost, and its photoefficiency can be promoted by the presence of hydrogen donor amine [15]. Two ways may be used to achieve type II polymeric photoinitiator systems: one is to use the polymeric photoinitiators and polymeric coinitiator amines [7], however, the polymer-bound photoinitiators or amines may show significantly decreased reactivity due to their poor diffusion ability; the other is to incorporate the photoinitiators and coinitiator amines into the same polymer chain, and it has obvious advantages such as efficient energy migration or intramolecular reactions to afford more reactive species, which can be protected as in a cage by the microenvironment of the polymer chain [4,7].

Recently, there has been extensive interest on aromatic ketone systems containing thio functionalities [6,16–20],

---

* Corresponding author. Tel.: +86 21 54743268; fax: +86 21 54747445.
E-mail address: jyin@sjtu.edu.cn (J. Yin).

1010-6030/$ – see front matter © 2006 Elsevier B.V. All rights reserved.
doi:10.1016/j.jphotochem.2006.07.020

probably because of the two advantages below: firstly, the thio atom may greatly red shift their absorption maxima [17]; secondly, aside from the H-abstraction reaction, these photoinitiators may also undergo photolysis reactions at the C–S bond as in type I systems [18]. Such increased absorption maximal and the photolysis reaction at C–S bond may greatly enhance their photoefficiency [16]. To our knowledge, however, there are few studies on sulfur-containing polymeric aromatic ketone systems [21].

In our previous work [22,23], we have synthesized three novel polymerizable sulfur-containing BP photoinitiators, 4-[(4-methacrylamido)thiophenyl]benzophenone (MAATPBP), 4-chloro-4′-[(4-methacrylamido)thiophenyl]benzophenone (CMAATPBP) and 4,4′-bis[(4-methacrylamido)thiophenyl]benzophenone (BMAATPBP), which are particularly attractive due to ease of synthesis and their high photoefficiency. In this paper, we report synthesis and some preliminar characterizations concerning the photoefficiency of a series of polymeric sulfur-containing photoinitiators bearing side-chain BP moiety and/or the coinitiator *N*,*N*-dimethylaminoethyl methacrylate (DMAEMA) group. Two copolymeric photoinitiators bearing side-chain BP and DMAEMA, P(MAATPBP-*co*-DMAEMA) and P(CMAATPBP-*co*-DMAEMA), were synthesized through copolymerization. The corresponding homopolymers, P(DMAEMA), P(MAATPBP) and P(CMAATPBP) were also prepared in order to compare the photoefficiency of the copolymers with their homopolymer counterparts. The most commercially used photoinitiator BP and their corresponding low molecular weight compounds (MAATPBP/DMAEMA and CMAATPBP/DMAEMA) were selected as the reference to evaluate their photoefficiency. UV–vis spectra and photopolymerization of difunctional 1,6-hexanediol diacrylate (HDDA) and trifunctional trimethylolpropane triacrylate (TMPTA) by photo-DSC were studied to investigate their photochemical behavior.

2. Experimental

2.1. Materials

2,2′-Azo-bis-isobutyronitrile (AIBN), 1,4-dioxane (DOX), *N*,*N*-dimethyl formamide (DMF) (from Medicine Group of China), *N*,*N*-dimethylaminoethyl methacrylate (DMAEMA) (from Shanghai Well Tone Material Company), 1,6-hexanediol diacrylate (HDDA) (from Kewang Chemical Reagent Company), trimethylolpropane triacrylate (TMPTA) (from Nantong Litian Chemical Company) were used as received. 4-[(4-Methacrylamido)thiophenyl]benzophenone (MAATPBP) and 4-chloro-4′-[(4-methacrylamido)thiophenyl]benzophenone (CMAATPBP) were synthesized according to our previous work [22,23]. Other chemicals are of analytical grade except as noted.

2.2. Synthesis of polymers

Three homopolymers of P(DMAEMA), P(MAATPBP), P(CMAATPBP), and two copolymers of P(MAATPBP-*co*-DMAEMA), P(CMAATPBP-*co*-DMAEMA), were prepared by thermal radical polymerization using AIBN as initiator. All polymerizations were carried out in a 25 mL glass vials, using 1.0 wt.% AIBN (w/w) with respect to monomers, and DMF (except for P(DMAEMA) with DOX) as the solvent. The monomers and AIBN were submitted to several freeze-thaw cycles before closing the vials. After sealing under high vacuum, the vials were kept at 85–90 °C for 72 h in the dark. The polymeric product was isolated by pouring the reaction mixture into a large excess of methanol (except for P(DMAEMA) with petroleum ether). After filtration, the polymers were dried under vacuum to constant weight and stored in the dark. The FT-IR and ^{1}H NMR confirmed the expected structures.

P(DMAEMA): ^{1}H NMR (CDCl$_3$, 400 MHz): $\delta = 3.96$ (2H, CH$_2$ of $-\underline{H_2C}-\overset{CH_3}{\overset{|}{C}}-\overset{O}{\overset{\|}{C}}-O-$), 2.49 (2H, CH$_2$ of CH$_2$O), 2.20 (6H, CH$_3$), 1.98–1.58 (2H, CH$_2$ of $-O-CH_2-\underline{CH_2}-$), 1.04–0.56 (3H, CH$_3$). FT-IR (KBr, cm^{-1}): 2947, 2821, 2770 (CH$_3$, CH$_2$), 1732 (C=O of $-O-\overset{O}{\overset{\|}{C}}-$).

P(MAATPBP): ^{1}H NMR (CDCl$_3$, 400 MHz): $\delta = 7.77$–6.88 (13H, aromatic), 2.09–1.78 (1H, CH of $-\underline{H_2C}-\overset{CH_3}{\overset{|}{C}}-\overset{O}{\overset{\|}{C}}-\overset{H}{N}-$), 1.76–1.40 (1H, CH of $-\underline{H_2C}-\overset{CH_3}{\overset{|}{C}}-\overset{O}{\overset{\|}{C}}-\overset{H}{N}-$), 1.36–0.75 (3H, CH$_3$). FT-IR (KBr, cm^{-1}): 3365 (NH), 1653 (C=O of $-\overset{H}{N}-\overset{O}{\overset{\|}{C}}-$), 1587 (C=C of Ar), 1081 (C–S).

P(CMAATPBP): ^{1}H NMR ([-d_6] DMSO, 400 MHz): $\delta = 8.39$–6.87 (12H, aromatic), 3.32–3.28 (1H, CH of $-\underline{H_2C}-\overset{CH_3}{\overset{|}{C}}-\overset{O}{\overset{\|}{C}}-\overset{H}{N}-$), 1.95–1.84 (1H, CH of $-\underline{H_2C}-\overset{CH_3}{\overset{|}{C}}-\overset{O}{\overset{\|}{C}}-\overset{H}{N}-$), 1.45–0.70 (3H, CH$_3$). FT-IR (KBr, cm^{-1}): 3364 (NH), 1658 (C=O of $-\overset{H}{N}-\overset{O}{\overset{\|}{C}}-$), 1588 (C=C of Ar), 1081 (C–S).

P(MAATPBP-*co*-DMAEMA): ^{1}H NMR (CDCl$_3$, 400 MHz): $\delta = 7.68$–7.10 (13H, aromatic), 5.74 (1H, CH of $-\underline{H_2C}-\overset{CH_3}{\overset{|}{C}}-\overset{O}{\overset{\|}{C}}-O-$), 5.43 (1H, CH of $-\underline{H_2C}-\overset{CH_3}{\overset{|}{C}}-\overset{O}{\overset{\|}{C}}-O-$), 3.98 (2H, CH$_2$ of CH$_2$O), 2.48 (2H, CH$_2$ of $-O-CH_2-\underline{CH_2}-$), 2.20–2.15 (1H, CH of $-\underline{H_2C}-\overset{CH_3}{\overset{|}{C}}-\overset{O}{\overset{\|}{C}}-\overset{H}{N}-$, 6H, CH$_3$ of –N–(CH$_3$)$_2$), 2.00 (1H, CH of $-\underline{H_2C}-\overset{CH_3}{\overset{|}{C}}-\overset{O}{\overset{\|}{C}}-\overset{H}{N}-$), 1.94–1.58 (3H, CH$_3$ of $-\underline{H_2C}-\overset{CH_3}{\overset{|}{C}}-\overset{O}{\overset{\|}{C}}-\overset{H}{N}-$), 1.49–0.74 (3H, CH$_3$ of $-\underline{H_2C}-\overset{CH_3}{\overset{|}{C}}-\overset{O}{\overset{\|}{C}}-O-$). FT-IR (KBr, cm^{-1}): 3526, 3353 (NH), 1731 (C=O of $-O-\overset{O}{\overset{\|}{C}}-$), 1682 (C=O of $-\overset{H}{N}-\overset{O}{\overset{\|}{C}}-$), 1659 (C=O of $-\overset{H}{N}-\overset{O}{\overset{\|}{C}}-$: hydrogen bond), 1652 ($Ar-\overset{O}{\overset{\|}{C}}-Ar$), 1588 (C=C of Ar), 1081 (C–S).

P(CMAATPBP-*co*-DMAEMA): ^{1}H NMR (CDCl$_3$, 400 MHz): $\delta = 7.68$–7.10 (12H, aromatic), 5.75 (1H, CH of $-\underline{H_2C}-\overset{CH_3}{\overset{|}{C}}-\overset{O}{\overset{\|}{C}}-O-$), 5.44 (1H, CH of $-\underline{H_2C}-\overset{CH_3}{\overset{|}{C}}-\overset{O}{\overset{\|}{C}}-O-$), 3.98 (2H, CH$_2$ of CH$_2$O), 2.96 (CH of $-\underline{H_2C}-\overset{CH_3}{\overset{|}{C}}-\overset{O}{\overset{\|}{C}}-\overset{H}{N}-$), 2.49 (2H, CH$_2$ of $-O-CH_2-\underline{CH_2}-$), 2.21–2.16 (6H, CH$_3$ of –N–(CH$_3$)$_2$), 2.01 (1H, CH of $-\underline{H_2C}-\overset{CH_3}{\overset{|}{C}}-\overset{O}{\overset{\|}{C}}-\overset{H}{N}-$), 1.95–1.59 (3H, CH_3 of $-\underline{H_2C}-\overset{CH_3}{\overset{|}{C}}-\overset{O}{\overset{\|}{C}}-\overset{H}{N}-$), 1.48–0.72 (3H, CH_3 of $-\underline{H_2C}-\overset{CH_3}{\overset{|}{C}}-\overset{O}{\overset{\|}{C}}-O-$). FT-IR (KBr, cm^{-1}): 3336 (NH), 1731 (C=O of $-O-\overset{O}{\overset{\|}{C}}-$), 1682 (C=O of $-\overset{H}{N}-\overset{O}{\overset{\|}{C}}-$), 1659 (C=O of $-\overset{H}{N}-\overset{O}{\overset{\|}{C}}-$: hydrogen bond), 1652 ($Ar-\overset{O}{\overset{\|}{C}}-Ar$), 1588 (C=C of Ar), 1081 (C–S).

2.3. Measurement

2.3.1. Physicochemical measurements

^{1}H NMR spectra were recorded on a Mercury Plus 400 MHz spectrometer with DMSO-d_6 or $CDCl_3$ as solvent.

FT-IR spectra were recorded on a Perkin-Elmer Paragon1000 FTIR spectrometer. The samples were prepared as KBr disc.

Elemental analysis was conducted on an Elementary Varioel apparatus.

UV–vis spectra were recorded in chloroform solution by a Perkin-Elmer Lambda 20 UV–vis spectrophotometer.

Molecular weights were determined by gel permeation chromatography (GPC) in THF solution on a Perkin-Elmer Series 200 apparatus. Monodisperse polystyrene (PS) samples were used as calibration standards.

2.3.2. Photocalorimetry (photo-DSC)

Photopolymerization of HDDA and TMPTA was studied by DSC 6200 (Seiko Instrument Inc.) photo-DSC with a high-pressure Hg lamp. The intensity of the light was measured by an Ultraviolet Radiometer (UIT-101), and the distance between the light source and the surface of the samples was 3 cm. Approximately 1.2 mg sample mixture was placed in the aluminum DSC pans.

Heat flow versus time (DSC thermogram) curves were recorded in an isothermal mode under a nitrogen flow of 50 mL/min. The reaction heat liberated in the polymerization was directly proportional to the number of vinyl groups reacted in the system (only a trace of polymerizable photoinitiator system was used compared with HDDA or TMPTA which can be omitted here). By integrating the area under the exothermic peak, the conversion of the vinyl groups (C) or the extent of reaction could be determined according to:

$$C = \frac{\Delta H_t}{\Delta H_0^{\mathrm{theor}}} \tag{1}$$

where ΔH_t is the reaction heat evolved at time t, and $\Delta H_0^{\mathrm{theor}}$ is the theoretical heat for complete conversion. $\Delta H_0^{\mathrm{theor}} = 86\,\mathrm{kJ/mol}$ for an acrylic double bond [24]. The rate of polymerization (R_p) is directly related to the heat flow (dH/dt) by the following equation:

$$R_p = \frac{dC}{dt} = \frac{dH/dt}{\Delta H_0^{\mathrm{theor}}} \tag{2}$$

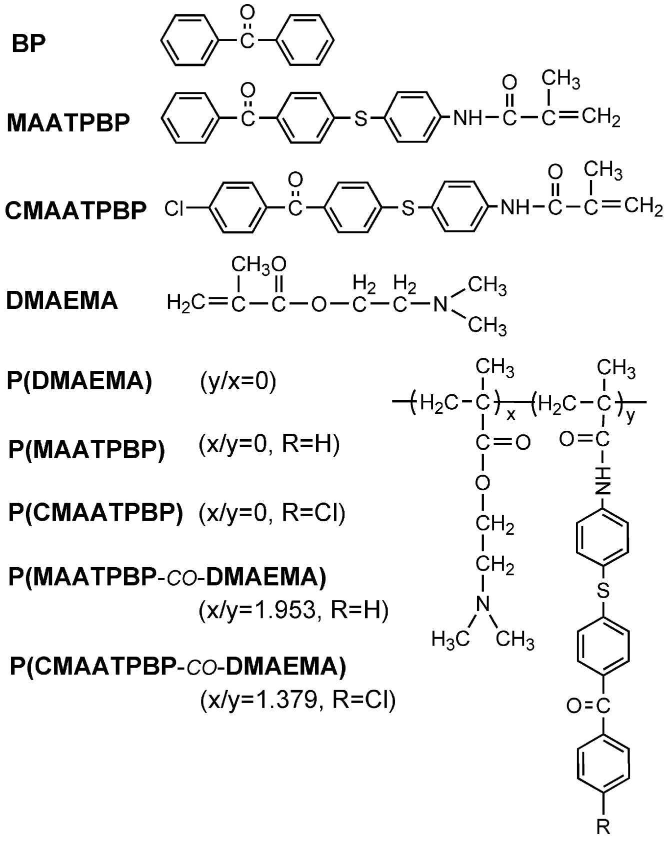

Scheme 1. Structure of photoinitiators and coinitiator DMAEMA.

3. Results and discussion

3.1. Synthesis and characterization of photosensitive polymers

The purpose of this paper is to provide a new way to achieve highly efficient sulfur-containing polymeric BP photoinitiators. The synthetical pathway leading to polymeric derivatives involves the preparation of the corresponding methacrylic monomers [23], successively submitted to radical homo- (P(DMAEMA), P(MAATPBP), P(CMAATPBP)) and copolymerization (P(MAATPBP-*co*-DMAEMA), P(CMAATPBP-*co*-DMAEMA)), in the presence of AIBN as shown in Scheme 1. Through the copolymerization of polymerizable photoinitiators of MAATPBP, CMAATPBP with the unsaturated coinitiator of DMAEMA, two novel sulfur-containing polymeric photoinitiators bearing side-chain BP and coinitiator amine were synthesized. In order to compare the photoefficiency of the copolymers with that of the corresponding homopolymers mixtures in photopolymerization, P(DMAEMA), P(MAATPBP) and P(CMAATPBP) were also prepared. Relevant synthesis and characterization data of the polymeric derivatives are summarized in Table 1.

^{1}H NMR and FT-IR spectra analysis of the polymers confirmed the expected structures. Indeed, ^{1}H NMR spectra (Figs. 1 and 2) of the two copolymers show the signals in the 4.0–2.4 ppm region given by the methylene protons in DMAEMA and in the region 7.0–8.0 ppm give by aromatic

Table 1
Synthesis and characterization data for polymeric photoinitiators

Sample	Feed (molar ratio), initiator/coinitiator	Product[a] (molar ratio), initiator/coinitiator	M_n[b] (g mol^{-1})	$M_\mathrm{w}/M_\mathrm{n}$[b]
P(DMAEMA)	0:1	0:1	295800	1.511
P(MAATPBP)	1:0	1:0	14560	1.346
P(MAATPBP-*co*-DMAEMA)	1:2	1:1.953	24220	1.455
P(CMAATPBP)	1:0	1:0	37500	1.141
P(CMAATPBP-*co*-DMAEMA)	1:2	1:1.379	63430	1.816

[a] Determined by elemental analysis.
[b] Determined by GPC.

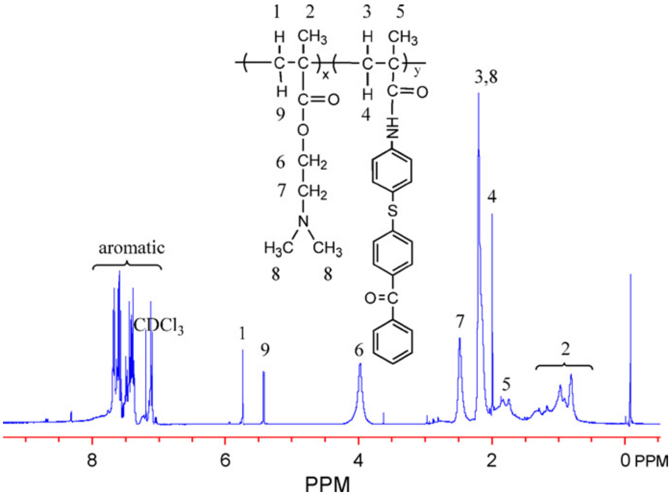

Fig. 1. ^{1}H NMR spectra of P(MAATPBP-*co*-DMAEMA) in CDCl$_3$.

protons in MAATPBP or CMAATPBP, thus clearly indicating that the polymerization reaction has involved the above unsaturated monomers. Figs. 1 and 2 further interpret each signal of the copolymeric photoinitiators in ^{1}H NMR. Accordingly, aside from the absorption of carbonyl groups from benzophenone (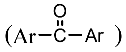 $\mathrm{Ar{-}C({=}O){-}Ar}$) at 1652 cm^{-1} in the FT-IR spectra of the copolymers, the signal of other carbonyl groups around 1659–1731 cm^{-1} from amido groups (C=O of 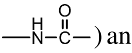 $\mathrm{{-}NH{-}C({=}O){-}}$) and urethano groups (C=O of 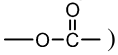 $\mathrm{{-}O{-}C({=}O){-}}$) verified that both DMAEMA and MAATPBP or CMAATPBP were successfully introduced into the macromolecular backbones.

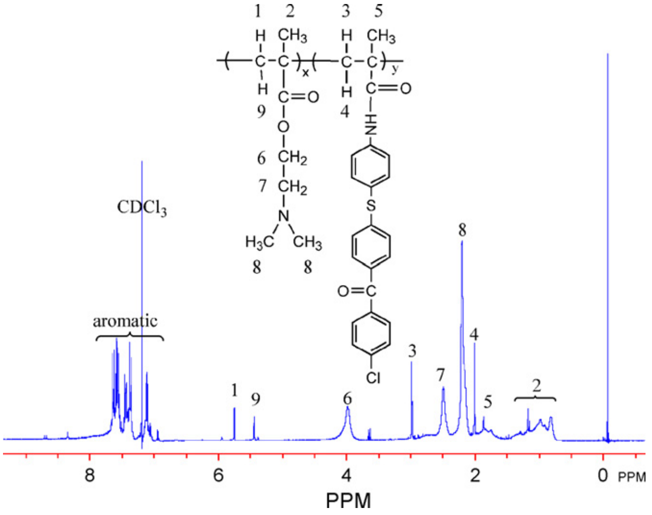

Fig. 2. ^{1}H NMR spectra of P(CMAATPBP-*co*-DMAEMA) in CDCl$_3$.

The average molecular weight obtained for the homopolymers and copolymers was determined by GPC. From Table 1, the average molecular weight values of P(MAATPBP-*co*-DMAEMA) and P(CMAATPBP-*co*-DMAEMA) are intermediate to those found for P(DMAEMA) and P(MAATPBP) or P(CMAATPBP), thus indicating there might be chain transfer and/or termination reactions involving amide groups for the monomers. The component of copolymers was determined by elemental analysis, by calculating the content of sulfur in copolymers. With respect to the corresponding feeds with the same molar ratio of initiator and coinitiator, however, P(MAATPBP-*co*-DMAEMA) displays a higher content of DMAEMA co-units than that in P(CMAATPBP-*co*-DMAEMA), thus suggesting a higher reactivity ratio of MAATPBP as compared with CMAATPBP.

3.2. *UV–vis spectra*

UV absorption spectra of MAATPBP, P(MAATPBP), P(MAATPBP-*co*-DMAEMA), CMAATPBP, P(CMAATPBP) and P(CMAATPBP-*co*-DMAEMA) were measured in chloroform using BP as the reference. Their maximal absorption ($\lambda_{\max}$) and the logarithmic values of molar extinction coefficient at $\lambda_{\max}$ (log ε) are summarized in Table 2. The longest wavelength absorption maximal for the compounds is important to their photoefficiency.

Transitions of BPs in the region of 250–300 nm are well known to belong to the main benzenoid π–π^* type transitions [25]. The n–π^* type transitions are usually found between 300 and 350 nm because of the spin forbidden transition [26]. The important consequence is that the molar extinction coefficient of n–π^* transitions are considerately weaker than that of π–π^* type transitions. Compared with BP, these polymerizable and polymeric sulfur-containing photoinitiators exhibit significantly red-shifted π–π^* maximal absorption. The introduction of thiophenyl groups markedly red shifts their main absorption maximum to above 300 nm due to increased electron donation via the sulfur atom [19]. This would certainly account for their increased photochemical activity during the photopolymerization.

Table 2
Absorption properties of BP, MAATPBP, P(MAATPBP), P(MAATPBP-*co*-DMAEMA), CMAATPBP, P(CMAATPBP), P(CMAATPBP-*co*-DMAEMA) in chloroform solution

Photoinitiator[a]	λ_{max} (nm)	$\log \varepsilon$ ($mol^{-1} cm^{-1} L$)
BP	254	4.286
MAATPBP	251 317	4.369 4.322
P(MAATPBP)	251 319	4.411 4.279
P(MAATPBP-*co*-DMAEMA)	251 317	4.382 4.307
CMAATPBP	256 321	4.371 4.333
P(CMAATPBP)	257 323	4.319 4.241
P(CMAATPBP-*co*-DMAEMA)	258 323	4.340 4.301

[a] The photoinitiator concentration is 5×10^{-5} M in terms of benzophenone moieties.

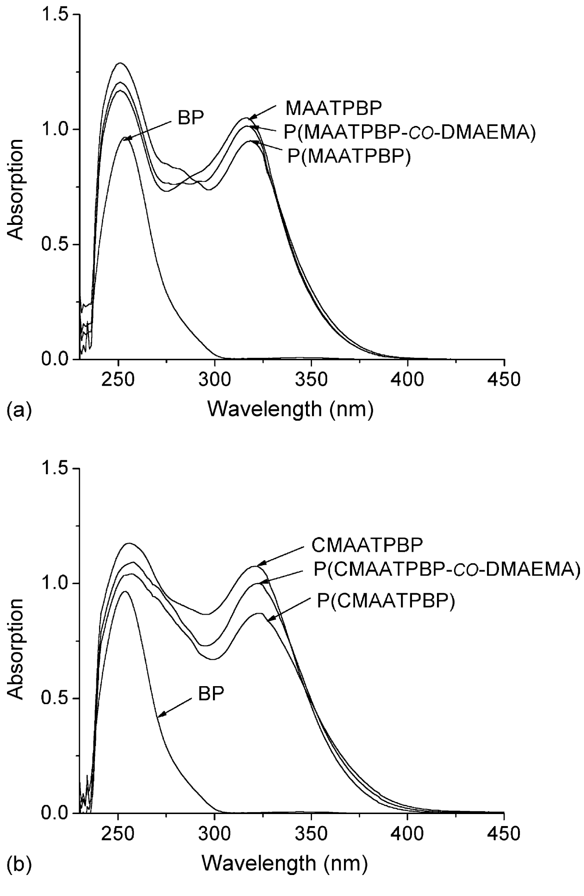

Fig. 3. UV–vis absorption spectra in chloroform solution with the concentration of 5×10^{-5} M (a) BP, MAATPBP, P(MAATPBP) and P(MAATPBP-*co*-DMAEMA); (b) BP, CMAATPBP, P(CMAATPBP) and P(CMAATPBP-*co*-DMAEMA).

From Fig. 3, polymeric photoinitiators exhibit the usual characteristic absorption in comparison with their monomers, which shows that the macromolecular structure and coinitiator amine have no significant influence on the UV–vis maximal absorption of BP moieties. However, with the disappearance of the carbon–carbon double bonds in P(MAATPBP) and P(CMAATPBP), their $\log \varepsilon$ value seems to decrease. Accordingly, the copolymers of P(MAATPBP-*co*-DMAEMA) and P(CMAATPBP-*co*-DMAEMA) exhibited an intermediate $\log \varepsilon$ value in comparison with their homopolymers and monomers. These may be due to the disappearance of the carbon–carbon double bonds in polymers, which lessens the conjugation of the polymers [27].

3.3. Photopolymerization of HDDA

Figs. 4 and 5 exhibit the photo-DSC profiles of HDDA initiated by these polymeric photoinitiators and their corresponding monomers (with the same molar ratio of BP/DMAEMA units). The results verify polymeric photoinitiators can efficiently initi-

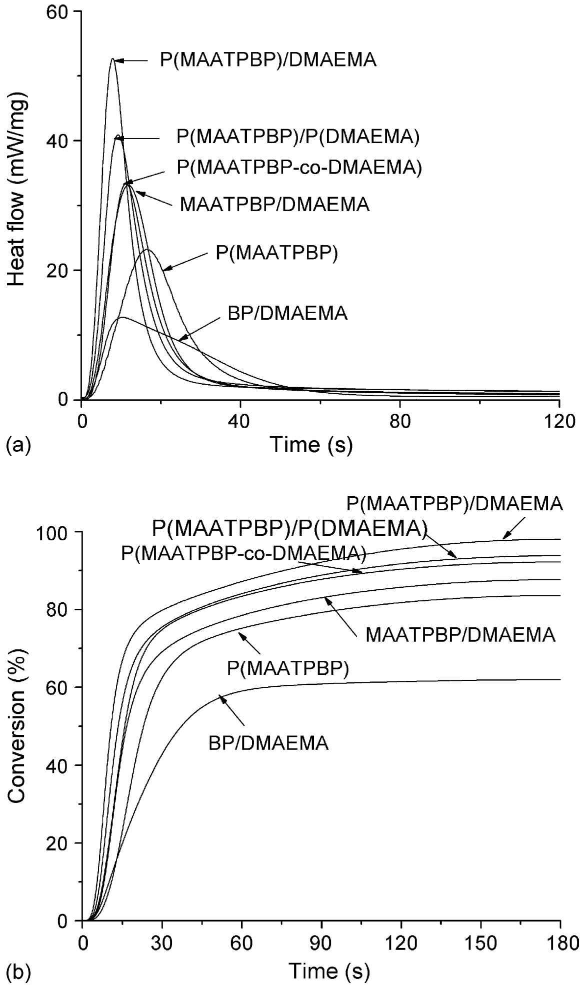

Fig. 4. (a) Heat flow vs. time; (b) conversion vs. time for polymerization of HDDA initiated by BP/DMAEMA, MAATPBP/DMAEMA, P(MAATPBP), P(MAATPBP)/DMAEMA, P(MAATPBP)/P(DMAEMA) and P(MAATPBP-*co*-DMAEMA), cured at 25 °C by UV light with an intensity of $55\,mW/cm^2$ (the photoinitiator concentration is 0.04 M in terms of benzophenone moieties with the same concentration of DMAEMA moieties).

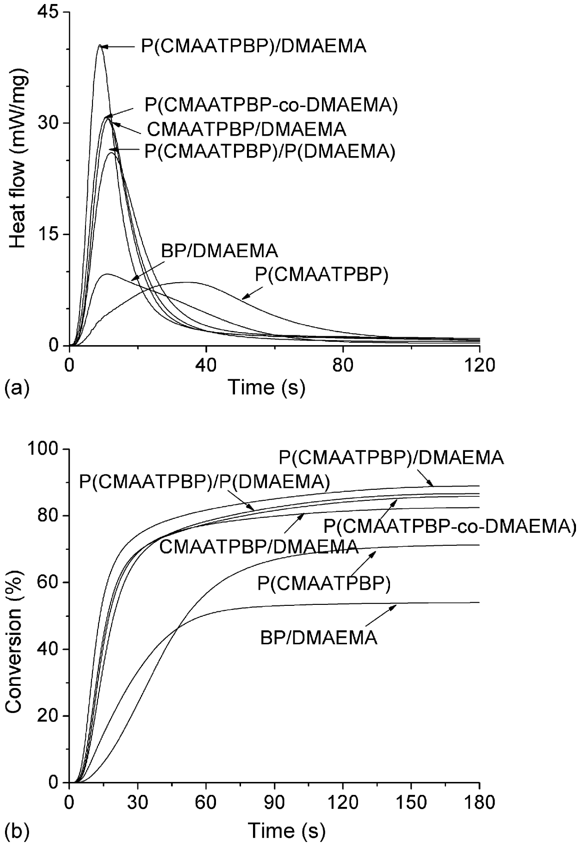

Fig. 5. (a) Heat flow vs. time; (b) conversion vs. time for polymerization of HDDA initiated by BP/DMAEMA, CMAATPBP/DMAEMA, P(CMAATPBP), P(CMAATPBP)/DMAEMA, P(CMAATPBP)/P(DMAEMA) and P(CMAATPBP-*co*-DMAEMA), cured at 25 °C by UV light with an intensity of 55 mW/cm^2 (the photoinitiator concentration is 0.04 M in terms of benzophenone moieties with the same concentration of DMAEMA moieties).

ate the photopolymerization and their behavior appears similar to other multifunctional monomers [15,26,28,29]. The crosslinking of HDDA studied by photo-DSC is a very rapid process, in which gelation often occurs at an early stage of the reaction. The formation of such gel structure may restrict the diffusion and mobility of radicals [30], thus resulting in a very short time to reach the maximal polymerization rate ($R_{\mathrm{p\,max}}$).

The photolysis of BP, in the presence of DMAEMA, leads to the formation of a radical produced from a carbonyl compound (ketyl-type radical) and another radical derived from coinitiators [31,32]. The ketyl radicals are usually not reactive toward vinyl monomers because of the steric hindrance and the delocalization of unpaired electron [3]. Meanwhile, aside from the bimolecular H-abstraction reaction between sulfur-containing BP derivatives and DMAEMA, the photolysis reaction at the C–S bond would certainly account for their photoefficiency [6,16–20]. The overall photoinitiation mechanism is presented in Scheme 2, from which we can know that the activity and the quantity of radicals (1)–(6) will mainly determine the photopolymerization rate. As for BP itself, the inactive radical from carbonyl compound will not participate in the photopolymerization. Therefore, the introduction of C–S bond and BP chromophore into polymers may greatly reduce the migration of species.

Table 3
Photopolymerization of HDDA initiated by BP/DMAEMA, MAATPBP/DMAEMA, P(MAATPBP), P(MAATPBP)/DMAEMA, P(MAATPBP)/P(DMAEMA) and P(MAATPBP-*co*-DMAEMA), cured at 25 °C by UV light with an intensity of 55 mW/cm^2

Photoinitiator[a]	$R_{\mathrm{p\,max}} \times 10^2$ (s^{-1})	Final conversion (%)	$T_{\max}$ (s)
BP/DMAEMA	2.045	61.96	10.4
MAATPBP/DMAEMA	5.437	87.66	11.2
P(MAATPBP)	3.745	83.59	16.6
P(MAATPBP)/DMAEMA	8.517	98.06	7.8
P(MAATPBP)/P(DMAEMA)	6.588	93.83	9.2
P(MAATPBP-*co*-DMAEMA)	5.376	92.20	11.8

[a] The photoinitiator concentration is 0.04 M in terms of benzophenone moieties with the same concentration of DMAEMA moieties.

From Tables 2 and 3, several conclusions can be drawn: firstly, P(MAATPBP) and P(CMAATPBP) can initiate the photopolymerization without coinitiator, because of the photolysis reaction at the C–S bond. Secondly, P(MAATPBP) is more efficient than BP/DMAEMA system different from that of P(CMAATPBP), thus indicating that higher active radicals generated at C–S bond in P(MAATPBP) than in P(CMAATPBP). Meanwhile, the efficiency of P(MAATPBP) and P(CMAATPBP) is much higher than that of their monomer counterparts in our previous work [23]. In case of the two homopolymers, polymer-bound radicals (1) and (3) may be protected from coupling reactions by the macromolecular coiling [33], thus increasing the initiation efficiency as compared with their low molecular counterparts. This result will greatly affect the photoefficiency of their polymeric combination with P(DMAEMA) or DMAEMA. Thirdly, copolymeric photoinitiators P(MAATPBP-*co*-DMAEMA) and P(CMAATPBP-*co*-DMAEMA) exhibit similar efficiency in comparison with their monomer combinations. Due to the steric hindrance of the macromolecular coil, macroradicals (1), (3), (5) and (6) generated from the copolymeric photoinitiators could unfavor recombination reactions between the propagating radicals, thus strongly limiting the extent of terminations and hence preventing a reduction of concentration of the active species [7]. Therefore, the efficiency of the copolymeric systems should be higher than that of the monomer combinations. However, the mobility of the polymeric amine component in copolymeric systems may be reduced, leading the similar photoefficiency of the copolymers compared with their monomer combinations. Another one is that, to our surprise, homopolymer combination of P(MAATPBP)/P(DMAEMA) is more efficient than P(MAATPBP-*co*-DMAEMA) different from that of P(CMAATPBP-*co*-DMAEMA) series. This result may be related to the photolysis reaction at C–S bond. The photolysis reaction at C–S bond might be easier to take place in their homopolymers than that of their copolymeric counterparts due to the bimolecular H-abstraction reaction in the same copolymeric chain. Thus, the photoefficiency of homopolymer combination of P(MAATPBP)/P(DMAEMA) is higher than P(MAATPBP-*co*-DMAEMA). As can be seen from Tables 3 and 4, the maximal initiation rate ($R_{\mathrm{p\,max}}$) of P(MAATPBP) is almost three times as much as that of P(CMAATPBP), thus the effect of the component of CMAATPBP on P(CMAATPBP-*co*-DMAEMA) may be

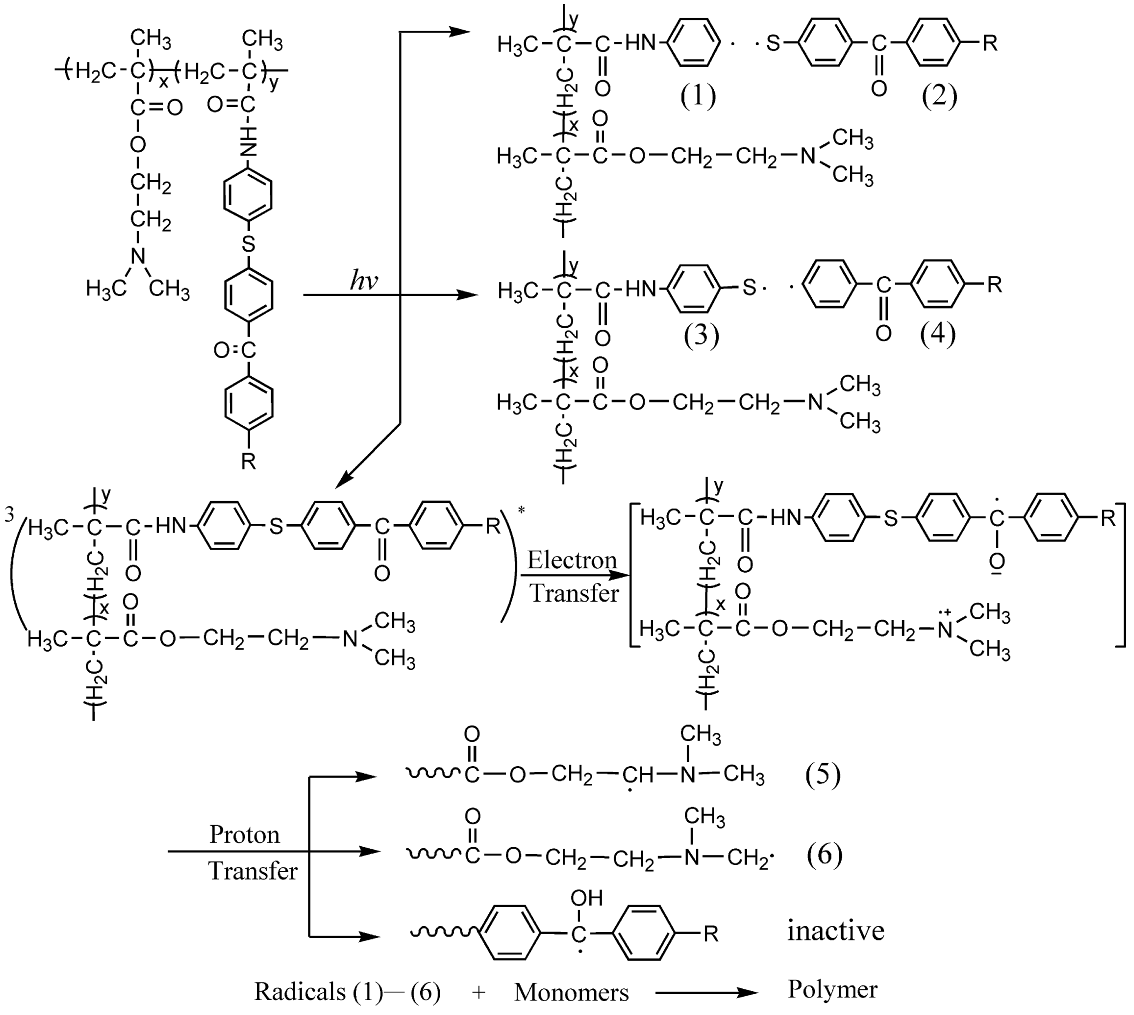

Scheme 2. Proposed initiation mechanisms for polymeric photoinitiators.

smaller than that of MAATPBP. Meanwhile, P(MAATPBP) or P(CMAATPBP) using DMAEMA as the coinitiator is more efficient than that of P(DMAEMA) as can be seen from Figs. 4 and 5. This result may be addressed to the reduced mobility of P(DMAEMA), leading to its poor diffusion ability and resulting in the decreased reactivity.

Notably, copolymeric sulfur-containing photoinitiators as well as their homopolymer combinations are highly efficient in which their $R_{\mathrm{p\,max}}$ is almost three times as high as that BP/DMAEMA system. It is a facile way to achieve polymeric photoinitiators while keeping high efficiency. This results may be addressed to two reasons: firstly, their red-shifted maximal absorption to BP; secondly, the photolysis reaction at C–S bond, thus leading to more active radicals generated from the photolysis at C–S bond. Figs. 4 and 5 further exhibit BP derivatives without coinitiator show lower photoefficiency than those in the presence of amine, which indicates that the coinitiator amine has obvious effect on the photoefficiency of polymeric photoinitiators.

Table 4
Photopolymerization of HDDA initiated by BP/DMAEMA, CMAATPBP/DMAEMA, P(CMAATPBP), P(CMAATPBP)/DMAEMA, P(CMAATPBP)/P(DMAEMA) and P(CMAATPBP-*co*-DMAEMA), cured at 25 °C by UV light with an intensity of 55 mW/cm^2

Photoinitiator[a]	$R_{\mathrm{p\,max}} \times 10^2$ (s^{-1})	Final conversion (%)	$T_{\max}$ (s)
BP/DMAEMA	1.563	53.99	11.0
CMAATPBP/DMAEMA	4.973	82.45	11.4
P(CMAATPBP)	1.371	71.23	34.4
P(CMAATPBP)/DMAEMA	6.573	88.95	8.8
P(CMAATPBP)/P(DMAEMA)	4.218	86.67	12.2
P(CMAATPBP-*co*-DMAEMA)	4.993	85.86	10.8

[a] The photoinitiator concentration is 0.04 M in terms of benzophenone moieties with the same concentration of DMAEMA moieties.

3.4. Photopolymerization of TMPTA

In order to further reveal the effect of monomer viscosity on photopolymerization, a trifunctional monomer of TMPTA, was chosen to be initiated by the photoinitiators mentioned above. Figs. 6 and 7 exhibit the photo-DSC profiles of TMPTA. It is well known the bimolecular H-abstraction reaction is chemically controlled [31]. When the reaction continues, however, the increased cross-linking level may eventually limit the monomer mobility, and then the propagation and termination reaction may become diffusion controlled [3,34,35]. Compared with HDDA, both the

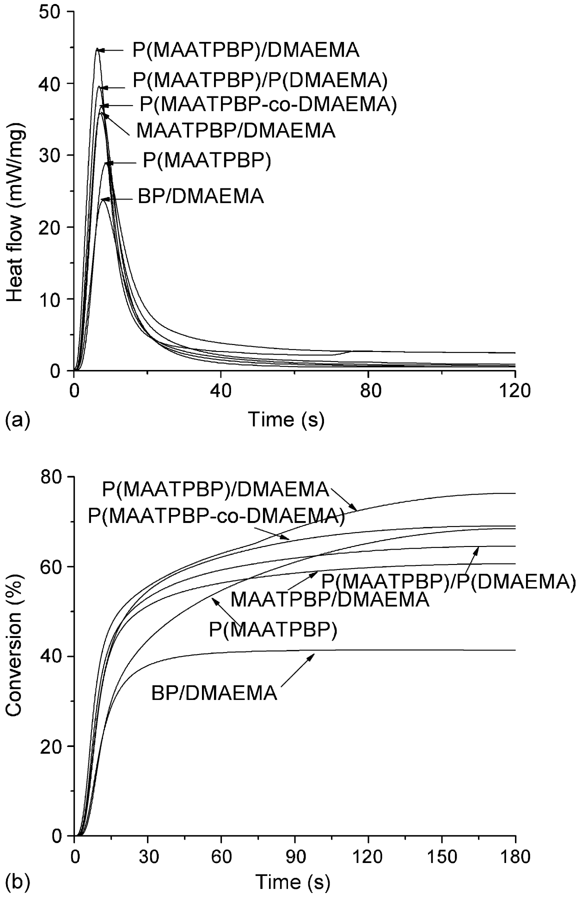

Fig. 6. (a) Heat flow vs. time; (b) conversion vs. time for polymerization of TMPTA initiated by BP/DMAEMA, MAATPBP/DMAEMA, P(MAATPBP), P(MAATPBP)/DMAEMA, P(MAATPBP)/P(DMAEMA) and P(MAATPBP-*co*-DMAEMA), cured at 25 °C by UV light with an intensity of 55 mW/cm^2 (the photoinitiator concentration is 0.04 M in terms of benzophenone moieties with the same concentration of DMAEMA moieties).

double bond content and the viscosity of TMPTA are much higher, thus leading to very high cross-linking density in the whole polymerization process of TMPTA [30]. The increased mobility of the system at lower viscosity delays the stage at which propagation becomes diffusion limited. Therefore, the time to reach the $R_{\mathrm{p\,max}}$ ($T_{\max}$) in TMPTA is shorter than that in HDDA as shown in Tables 5 and 6.

Table 5
Photopolymerization of TMPTA initiated by BP/DMAEMA, MAATPBP/DMAEMA, P(MAATPBP), P(MAATPBP)/DMAEMA, P(MAATPBP)/P(DMAEMA) and P(MAATPBP-*co*-DMAEMA), cured at 25 °C by UV light with an intensity of 55 mW/cm^2

Photoinitiator[a]	$R_{\mathrm{p\,max}} \times 10^2$ (s^{-1})	Final conversion (%)	$T_{\max}$ (s)
BP/DMAEMA	3.291	41.40	8.0
MAATPBP/DMAEMA	5.137	60.62	7.4
P(MAATPBP)	3.543	68.48	8.6
P(MAATPBP)/DMAEMA	6.243	76.34	6.4
P(MAATPBP)/P(DMAEMA)	5.536	64.55	6.8
P(MAATPBP-*co*-DMAEMA)	5.016	69.04	7.2

[a] The photoinitiator concentration is 0.04 M in terms of benzophenone moieties with the same concentration of DMAEMA moieties.

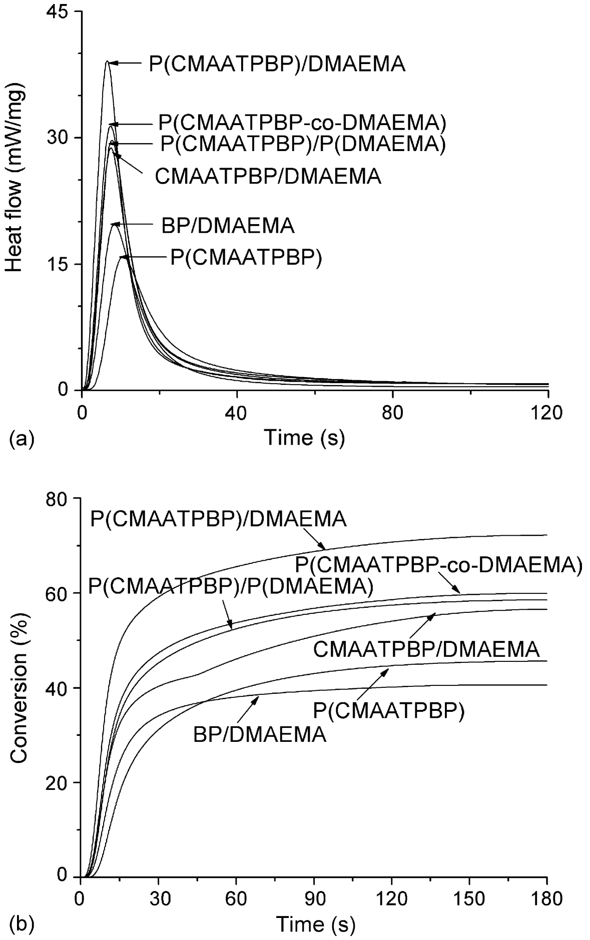

Fig. 7. (a) Heat flow vs. time; (b) conversion vs. time for polymerization of TMPTA initiated by BP/DMAEMA, CMAATPBP/DMAEMA, P(CMAATPBP), P(CMAATPBP)/DMAEMA, P(CMAATPBP)/P(DMAEMA) and P(CMAATPBP-*co*-DMAEMA), cured at 25 °C by UV light with an intensity of 55 mW/cm^2 (the photoinitiator concentration is 0.04 M in terms of benzophenone moieties with the same concentration of DMAEMA moieties).

From Figs. 6 and 7, these copolymeric photoinitiators as well as their homopolymer combinations are still more efficient than BP/DMAEMA system, but some differences exist besides $T_{\max}$: firstly, compared with BP/DMAEMA system, the increment of their $R_{\mathrm{p\,max}}$ is smaller than in HDDA system, probably

Table 6
Photopolymerization of TMPTA initiated by BP/DMAEMA, CMAATPBP/DMAEMA, P(CMAATPBP), P(CMAATPBP)/DMAEMA, P(CMAATPBP)/P(DMAEMA) and P(CMAATPBP-*co*-DMAEMA), cured at 25 °C by UV light with an intensity of 55 mW/cm^2

Photoinitiator[a]	$R_{\mathrm{p\,max}} \times 10^2$ (s^{-1})	Final conversion (%)	$T_{\max}$ (s)
BP/DMAEMA	2.755	40.56	8.4
CMAATPBP/DMAEMA	3.983	56.55	7.4
P(CMAATPBP)	2.216	45.61	10.6
P(CMAATPBP)/DMAEMA	6.348	72.20	6.2
P(CMAATPBP)/P(DMAEMA)	4.145	58.52	7.8
P(CMAATPBP-*co*-DMAEMA)	4.382	59.92	7.4

[a] The photoinitiator concentration is 0.04 M in terms of benzophenone moieties with the same concentration of DMAEMA moieties.

in consequence of the reduced mobility of the polymeric photoinitiators in the higher viscosity reaction medium. Secondly, the final conversion is smaller than their counterparts in HDDA, thus verifying rapid cross-linking in TMPTA may limit their photopolymerization process. Thirdly, the differences between P(CMAATPBP-*co*-DMAEMA) and CMAATPBP/DMAEMA is enlarged. This result further indicates that the macromolecular structure of the BP and DMAEMA moieties may favor the possibility of efficient energy migration and intramolecular reactions.

4. Conclusions

In this article, we report the synthesis and some preliminar characterizations of a series of polymeric sulfur-containing photoinitiators bearing side-chain BP moiety and/or the coinitiator DMAEMA group. On the basis of the obtained results, the following concluding remarks can be drawn:

1. Novel copolymeric photoinitiators bearing side-chain BP and DMAEMA, such as P(MAATPBP-*co*-DMAEMA) and P(CMAATPBP-*co*-DMAEMA), and the corresponding homopolymers, P(DMAEMA), P(MAATPBP) and P(CMAATPBP), have been synthesized and fully characterized.
2. P(MAATPBP) and P(CMAATPBP) can efficiently initiate the photopolymerization without coinitiator because of the photolysis reaction at C–S bond. Polymer-bound radicals may be protected from coupling reactions by the macromolecular coiling, thus increasing their initiation efficiency as compared with their low molecular counterparts.
3. Copolymeric photoinitiators of P(MAATPBP-*co*-DMAEMA) and P(CMAATPBP-*co*-DMAEMA), as well as homopolymeric combinations, are much more efficient than BP/DMAEMA system.
4. The photolysis reaction at C–S bond greatly affects the bimolecular H-abstraction reaction in the copolymeric photoinitiators, thus decreasing the effect of interaction between BP and DMAEMA moiety in the same polymer chain and leading the higher efficiency of P(MAATPBP)/P(DMAEMA) in comparison with P(MAATPBP-*co*-DMAEMA).
5. The reduced mobility of the polymeric photoinitiators in the higher viscosity reaction medium of TMPTA shortens the stage at which propagation becomes diffusion limited, leading to its shorter time to reach $R_{\mathrm{p\,max}}$ and difficult to reach high final conversion.

Acknowledgements

The authors express their gratitude to the Ministry of Science and Technology of China (no: 2004AA33H010), and the Ministry Education of China (Kuashiji Scholar Project) for their financial support.

Appendix A. Supplementary data

Supplementary data associated with this article can be found, in the online version, at doi:10.1016/j.jphotochem.2006.07.020.

References

[1] T. Corrales, F. Catalina, C. Peinado, N.S. Allen, A.M. Rufs, C. Bueno, M.V. Encinas, Polymer 43 (2002) 4591–4597.
[2] C. Decker, C. Bianchi, S. Jönsson, Polymer 45 (2004) 5803–5811.
[3] X.S. Jiang, J. Yin, Macromol. Rapid. Commun. 25 (2004) 748–752.
[4] T. Corrales, F. Catalina, C. Peinado, N.S. Allen, J. Photochem. Photobiol. A: Chem. 159 (2003) 103–114.
[5] X.S. Jiang, J. Yin, Macromolecules 37 (2004) 7850–7853.
[6] L. Angiolini, D. Caretti, C. Carlini, E. Corell, E. Salatelli, Polymer 40 (1999) 7197–7207.
[7] L. Angiolini, D. Caretti, E. Salatelli, Macromol. Chem. Phys. 201 (2000) 2646–2653.
[8] C. Decker, Macromol. Rapid. Commun. 23 (2002) 1067–1093.
[9] C. Valderas, S. Bertolotti, C.M. Previtali, M.V. Encinas, J. Polym. Sci. Part A: Polym. Chem. 40 (2002) 2888–2893.
[10] C. Peinado, A. Alonso, E.F. Salvador, J. Baselga, C. Fernando, Polymer 43 (2002) 5355–5361.
[11] C. Decker, F. Morel, S. Jönsson, C. Hoyle, Macromol. Chem. Phys. 200 (1999) 1005–1013.
[12] C. Decker, C. Bianchi, F. Morel, S. Jönsson, C. Hoyle, Macromol. Chem. Phys. 201 (2000) 1493–1503.
[13] C. Carlini, F. Gurzoni, Polymer 24 (1983) 101–106.
[14] R.S. Davidson, H.J. Hageman, S.P. Lewis, J. Photochem. Photobiol. A: Chem. 118 (1998) 183–188.
[15] X.S. Jiang, J. Yin, J. Photochem. Photobiol. A: Chem. 174 (2005) 165–170.
[16] N.S. Allen, T. Corrales, M. Edge, F. Catalina, M. Bianco, A. Green, Polymer 39 (1998) 903–909.
[17] N.S. Allen, M. Edge, F. Catalina, T. Corrales, M. Bianco, A. Green, J. Photochem. Photobiol. A: Chem. 110 (1997) 183–190.
[18] N.S. Allen, T. Corrales, M. Edge, F. Catalina, M. Bianco, A. Green, Euro. Polym. J. 34 (1997) 303–308.
[19] J.P. Fouassier, D.J. Lougnot, L. Avar, Polymer 36 (1995) 5005–5010.
[20] J. Paczkowski, Z. Kucybala, F. Scigalski, A. Wrzyszczynski, J. Photochem. Photobiol. A: Chem. 159 (2003) 115–125.
[21] L. Angiolini, D. Caretti, C. Carlini, E. Corelli, J.P. Fouassier, F. Morlet-Savary, Polymer 36 (1995) 4055–4060.
[22] H.Y. Wang, J. Wei, X.S. Jiang, J. Yin, Polymer 47 (2006) 4967–4975.
[23] H.Y. Wang, J. Wei, X.S. Jiang, J. Yin, Macromol. Chem. Phys. 207 (2006) 1080–1086.
[24] E. Andrzejewska, M. Andrzejewski, J. Polym. Sci. Part A: Polym. Chem. 36 (1998) 665–673.
[25] R. Liska, J. Polym. Sci. Part A: Polym. Chem. 40 (2002) 1504–1518.
[26] S. Jauk, R. Liska, Macromol. Rapid. Commun. 26 (2005) 1687–1692.
[27] S.Y. Yu, J. Qiu, G.Q. Yao, Q.Y. Gao, G.X. Yang, J.X. Zhang, F.M. Li, J. Appl. Polym. Sci. 65 (1997) 481–489.
[28] X.S. Jiang, J. Yin, Polymer 45 (2004) 5057–5063.
[29] L. Lecamp, B. Youssef, C. Bunel, Polymer 40 (1999) 1403–1409.
[30] X.S. Jiang, H.J. Xu, J. Yin, Polymer 45 (2004) 133–140.
[31] F.S. Du, P. Zhang, F.M. Li, J. Appl. Polym. Sci. 51 (1994) 2139–2144.
[32] D.G. Anderson, J. Davidson, J.J. Elvery, Polymer 37 (1996) 2477–2484.
[33] C. Carlini, L. Angiolini, D. Caretti, E. Corelli, J. Appl. Polym. Sci. 64 (1997) 2237–2246.
[34] T.F. Scott, W.D. Cook, J.S. Forsythe, Polymer 43 (2002) 5839–5845.
[35] W.D. Cook, Polymer 33 (1992) 2152–2161.